MAD/PH/151
January 1984

THE PROCESS $e^+e^- \rightarrow q\bar{q}\gamma$ AND THE ELECTRIC CHARGE OF COLORED QUARKS

Jean René Cudell, Francis Halzen and Franz Herzog
Physics Department, University of Wisconsin, Madison, Wisconsin 53706

Abstract

Measurements involving more than one photon may determine the individual charges of colored quarks rather than the color-averaged value measured, for example, by the R-value in $e^+e^- \rightarrow$ hadrons. We investigate the process $e^+e^- \rightarrow q\bar{q}\gamma$ and find that ϕ-distributions, where ϕ is the azimuthal angle of the quark with respect to the γ-momentum, are very sensitive to the charge assignments of colored quarks. We study experimental implications and make comparisons with the process $qq \rightarrow qq\gamma$, taking place in hadron collision experiments.

With any charge assignment Q_R, Q_G, Q_B and Q_R-1, Q_G-1, Q_B-1 for colored quarks grouped in the usual generation pattern, we will reproduce the spectrum of colorless hadrons provided the condition

$$Q_R + Q_G + Q_B = 2 \tag{1}$$

holds.[1] As a consequence experiments measuring only the color-averaged quark charge $\langle Q \rangle$ cannot distinguish between different charge assignments for colored quarks. (For example, Gell-Mann-Zweig quarks with $Q_R = Q_G = Q_B = 2/3$ and Han-Nambu quarks with $Q_R = 0$, $Q_G = Q_B = 1$). Such experiments include the R-parameter in e^+e^- annihilation into hadrons, the ratio of Drell-Yan cross sections $\sigma(\pi^- A \to \gamma^* X)/\sigma(\pi^+ A \to \gamma^* X)$ on an isoscalar target A, the ratio of structure functions $F_2(ep)/F_2(en)$ and the average charge of leading hadrons in a jet. The standard example of experiments sensitive to the discriminating $\langle Q^2 \rangle$ rather than $\langle Q \rangle^2$ is the process $\gamma\gamma \to q\bar{q}$ (F.n. 1). It has been pointed out recently[2] that the goal of separating the charges of colored quarks can also be achieved by studying the hadronic process $qq' \to qq'\gamma$. The key observation is that the cross section not only depends on $\langle Q_q \rangle^2$ and $\langle Q_{q'} \rangle^2$ but also on an interference term $\langle Q_q Q_{q'} \rangle$ which is not fixed by condition (1). In specific channels like $u\bar{d} \to u\bar{d}\gamma$ and $uu \to uu\gamma$ the signature of this interference term is truly dramatic due to the presence of radiation zeroes.[3]

In this paper we study the two-photon process $e^+e^- \to q\bar{q}\gamma$. Experiments identifying $q\bar{q}\gamma$ final states are in progress and measurements of this type sense the proximity of a possible color threshold when exploring a new range of energies as will soon be feasible with the

LEP-collider. In a previous study Brodsky, Carlson and Suaya[4] suggested measuring the charge asymmetry of the final state hadrons h

$$A_h(z) \sim \frac{d\sigma(e^+e^- \to \gamma h X)}{(d^3k/k^o)d\Omega_h dz} - \frac{d\sigma(e^+e^- \to \gamma \bar{h} X)}{(d^3k/k^o)d\Omega_{\bar{h}} dz} \quad . \qquad (2)$$

Here k is the four-momentum of the photon and z the longitudinal momentum fraction of the hadron $h(\bar{h})$ in the parent $q(\bar{q})$ jet. This asymmetry is related by a sum rule[4] to $\langle Q^2 \rangle$ and its experimental evaluation is a formidable task. Now that data on the process are accumulating we find it important to shed new light on this problem. Especially we find that the azimuthal angle (ϕ) distribution of the quark with respect to the γ-momentum (see Fig. 1) is very sensitive to $\langle Q^2 \rangle$. We will conclude that the differential cross section $d\sigma/d\phi$ is experimentally accessible and that the rate, even with cuts, is sufficient to extract direct information on the charge of colored quarks. The difficulty of this task should be contrasted with the alternative experiment measuring the R-value in $\gamma\gamma \to$ hadrons.

We outline our calculation next. The amplitude for $e^-(p_1) + e^+(p_2) \to \gamma(k) + q(p_3) + \bar{q}(p_4)$ has the form

$$M = (\sqrt{4\pi\alpha})^2 \langle Q \rangle M_1 + \sqrt{4\pi\alpha}\, Q^2{}_{eff} M_2 \qquad (3)$$

where, up to charge factors, $M_1(M_2)$ is the amplitude for real photon emission from the lepton (quark) current. α is the fine structure constant and Q^2_{eff} is an effective charge square that carries information on a possible color threshold. In quantum chromodynamics (QCD) we have $Q^2_{eff} = \langle Q^2\rangle = \langle Q\rangle^2$. The cross section is given by:[5]

$$d\sigma = \frac{\alpha}{(8\pi)^2}\,\sigma_o\,\frac{t^2 + t'^2 + u^2 + u'^2}{s'}\,S\,dx_q dx_{\bar{q}} d\cos\theta_\gamma d\phi \qquad (4a)$$

where

$$S = \frac{s}{p_1\cdot k\;p_2\cdot k} + \frac{(Q^2_{eff})^2}{\langle Q\rangle^2}\,\frac{s'}{p_3\cdot k\;p_4\cdot k}$$

$$-\frac{\langle Q\rangle Q^2_{eff}}{\langle Q\rangle^2}\left\{\frac{t}{p_1\cdot k\;p_3\cdot k} + \frac{t'}{p_2\cdot k\;p_4\cdot k} - \frac{u}{p_1\cdot k\;p_4\cdot k} - \frac{u'}{p_2\cdot k\;p_3\cdot k}\right\} \qquad (4b)$$

and

$$\sigma_o = \frac{4\pi\alpha^2}{s}\langle Q\rangle^2 \qquad (4c)$$

is the $e^+e^- \to q\bar{q}$ annihilation cross section in lowest order QED that only probes $\langle Q\rangle^2$. The kinematics of the process is shown in Fig. 1; x_q and $x_{\bar{q}}$ are the energy fractions of the quark and antiquark in the e^+e^- center-of-mass system ($x_q = 2(p_3^o)_{cm}/\sqrt{s}$, $x_{\bar{q}} = 2(p_4^o)_{cm}/\sqrt{s}$). The generalized Mandelstam variables are defined as

$$\begin{aligned} s &= (p_1+p_2)^2 & s' &= (p_3+p_4)^2 \\ t &= (p_1-p_3)^2 & t' &= (p_2-p_4)^2 \\ u &= (p_1-p_4)^2 & u' &= (p_2-p_3)^2\,. \end{aligned} \qquad (5)$$

To understand the relevance of the quark azimuthal angle distribution as a probe of Q^2_{eff} we cast (4) into a more explicit form:

$$\frac{1}{\sigma_o}\frac{d\sigma}{dx_q dx_{\bar{q}} d\cos\theta_\gamma d\phi} = \frac{\alpha}{(8\pi)^2}\left[F_1 + F_2(1+\cos^2\theta_\gamma) + F_3\sin^2\theta_\gamma \right.$$

$$\left. + F_3\sin^2\theta_\gamma\cos 2\phi + F_4\sin 2\theta_\gamma\cos\phi\right]$$

$$\times\left[\frac{H_1}{\sin^2\theta_\gamma} + \frac{(Q^2_{eff})^2}{\langle Q\rangle^2} H_2 + \frac{Q^2_{eff}}{\langle Q\rangle}\frac{\cos\phi}{\sin\theta_\gamma} H_3\right] . \quad (6a)$$

The functions $F_1,\ldots,F_4$ and $H_1,\ldots,H_2$ are independent of the polar and azimuthal angle θ_γ and ϕ:

$$F_1 = \frac{x_q^2 + x_{\bar{q}}^2 - x_\gamma^2 - 2x_q^2\cos^2\theta_{\gamma q} - 2x_\gamma x_q\cos\theta_{\gamma q}}{2(1-x_\gamma)}$$

$$F_2 = \frac{x_\gamma^2 + 2x_q^2\cos^2\theta_{\gamma q} + 2x_\gamma x_q\cos\theta_{\gamma q}}{2(1-x_\gamma)}$$

$$(6b)$$

$$F_3 = \frac{x_q^2\sin^2\theta_{\gamma q}}{2(1-x_\gamma)}$$

$$F_4 = -\frac{x_q^2\sin 2\theta_{\gamma q} + x_q x_\gamma\sin\theta_{\gamma q}}{1 - x_\gamma}$$

and

$$H_1 = \frac{16}{x_\gamma^2} \qquad H_2 = \frac{4(1+x_q+x_\gamma)}{(1-x_q)(1-x_{\bar{q}})} \qquad H_3 = \frac{16\sqrt{(1-x_{\bar{q}})(x_\gamma x_q + x_{\bar{q}} - 1)}}{x_\gamma(1-x_q)(1-x_{\bar{q}})} . \quad (6c)$$

Here we use the notation $x_\gamma = 2 - x_q - x_{\bar{q}}$ and $\cos\theta_{\gamma q} = 1 - 2(x_\gamma + x_q - 1)/x_\gamma x_q$. Comparison of Eqs. (4b) and (6a) reveals that the interference term proportional to $Q^2_{eff}/\langle Q\rangle$, a direct measure of the quantity Q^2_{eff}, oscillates in the azimuthal angle ϕ. Indeed up to the overall factor $(F_1 + \ldots F_4)$ in (6a) only the interference term is responsible for the observed ϕ-dependence. It is thus clear that the Q^2_{eff}-dependent interference pattern in the azimuthal distribution $d\sigma/d\phi$ yields direct experimental information about the color dependence of quark charges. We note here that in the process $qq \to qq\gamma$ it is the $\cos\theta_\gamma$-distribution which is sensitive to the interference term due to the appearance of radiation zeroes. The measurement of this polar angle distribution is however not useful in the case of e^+e^- experiments as the structure in $d\sigma/d\cos\theta_\gamma$ is dominated by the charge independent term $H_1/\sin^2\theta_\gamma$, see Eq. (6a).

We support our claim with some illustrative calculations next. We impose the following cuts on the orientations of the final state particles:

$$|\cos\theta_\gamma| < .95\ , \quad |\cos\theta_q| < .95\ , \quad |\cos\theta_{\bar q}| < .95$$
$$|\cos\theta_{q\bar q}| < .95\ , \quad x_q > .2\ , \quad x_\gamma > .2\ . \tag{7}$$

$\theta_q(\theta_{\bar q})$ is the opening angle between the electron and the quark (antiquark) jet, $\theta_{q\bar q}$ the angle between the quark- and antiquark-jet in the e^+e^- c.m. frame. These cuts guarantee that the γ and the two jets can be separated and are not too close to the e^+e^- beams. They also cure mass- and infrared singularities and thus it is possible to make a direct comparison of the perturbative result (6) with data.

In Figs. 2 and 3 we show the ϕ-distribution for Gell-Mann-Zweig quarks ($Q_R = Q_G = Q_B$) with charges $Q = 2/3$ and $Q = 1/3$, respectively.

Separately shown are the interference term (-•-•-), non-interference term (- - -) as defined by (4b) and their sum (———). With this charge assignment we therefore have $\langle Q \rangle^2 = \langle Q^2 \rangle = Q^2_{eff}$. This is the standard QCD prediction and significant deviations from it would be an indication for a nearby color threshold. The structure seen in the separate curves for both the interference and non-interference terms is mainly due to the cuts (7). These figures clearly show the sensitivity of the ϕ-distribution to the quark charge. The magnitude of this term is substantial and thus the overall ϕ-distributions for the quark charges $Q = 2/3$ and $Q = 1/3$ are quite different, especially in respect to the slope in the regions $60^\circ \leq \phi \leq 180^\circ$ and $180^\circ \leq \phi \leq 300^\circ$. The ϕ-distribution for the quarks with charge $Q = -1/3$ can be obtained from the ϕ-distribution for $Q = 1/3$ in Fig. 3 by simply replacing $\phi \rightarrow \pi + \phi$; this is a consequence of charge conjugation invariance. In Fig. 4 we present a ϕ-distribution for a quark with $\langle Q \rangle = 2/3$ but now we consider different values for Q^2_{eff}, as suggested by broken color theories (F.n. 2). Separately shown are curves for $Q^2_{eff} = 1$(- - -), $Q^2_{eff} = 1/9$(-•-•-) and $Q^2_{eff} = 4/9$(———). For $Q^2_{eff} = 4/9$ we reproduce the Gell-Mann-Zweig result in Fig. 2). The striking dependence of $d\sigma/d\phi$ on the value of Q^2_{eff} is clearly illustrated.

We conclude with a final comment. Although the experiment we propose only requires the measurement of the orientation of the final γ and jet direction, discrimination of the q and $\bar{q}$ jet is necessary, because ϕ is defined with respect to the quark (not the antiquark) jet direction. It is sufficient to separate $q,\bar{q}$ statistically using either the charge of the leading particle or the average observed charge of the hadrons in each jet. An experiment lacking quark/antiquark identification would see a superposition of the distributions for $|Q|$ and $-|Q|$, as shown in Fig. 5, where curves for $|Q| = 2/3$(———) and for $|Q| = 1/3$(- - -) are shown. As may be seen from (6a), the ϕ-dependence of these distributions is not as strong as that shown in Figs. 2 and 3 and thus only a mild sensitivity on Q^2_{eff} survives.

Acknowledgments

We thank K. Hagiwara for reading the manuscript and K. Hagiwara, R. Prepost and P. Stevenson for helpful discussions.

This research was supported in part by the University of Wisconsin Research Committee with funds granted by the Wisconsin Alumni Research Foundation, and in part by the Department of Energy under contract DE-AC02-76ER00881.

REFERENCES

1. See, e.g., F. E. Close, An Introduction to Quarks and Partons (Academic Press, New York, 1979).
2. K. Hagiwara, F. Halzen and F. Herzog, Madison preprint MAD/PH/137, Phys. Lett. B (to be published).
3. S. J. Brodsky and R. W. Brown, Phys. Rev. Lett. 49, 966 (1982); M. A. Samuel, Phys. Rev. D27, 2724 (1983); R. W. Brown, K. L. Kowalski and S. J. Brodsky, Phys. Rev. D28, 624 (1983).
4. S. J. Brodsky, C. E. Carlson and R. Suaya, Phys. Rev. D14, 2264 (1976).
5. F. A. Berends, R. Kleiss, P. De Causmaecker, R. Gastmans and T. T. Wu, Phys. Lett. 103B, 124 (1981).

FOOTNOTES

F.n. 1 It has, however, been conjectured by Lipkin (H. J. Lipkin, Phys. Lett. 85B (1979) 236; Nucl. Phys. B155 (1979) 104) that far below color threshold every experiment is exclusively sensitive to $\langle Q \rangle$, independent of the number of photons involved. Only as the scale of a process approaches the scale of color threshold higher charge moments $\langle Q^n \rangle$, $n > 1$, that are due to higher order electromagnetic perturbations in the quark and gluon current, may start to be important. These infrared sensitive conjectures could not be proven rigorously for any theory (model).

F.n. 2 A complete calculation in a broken color gauge theory with Han-Nambu quarks should also consider radiation off charged gluons present in such theories. The values of $Q^2_{eff} \neq 4/9$ should be considered as "toy" values. For gauge theories where color is eventually unfrozen we refer to, e.g., J. C. Pati and A. Salam, Phys. Rev. Lett. 31 (1973) 661; Phys. Rev. D8 (1973) 1240.

FIGURE CAPTIONS

Fig. 1 Kinematics of the process $e^+e^- \to q\bar{q}\gamma$ in the e^+e^- center-of-mass frame. The $\bar{q}$ with momentum p_4 is not shown.

Fig. 2 ϕ-distribution for the process $e^+e^- \to q\bar{q}\gamma$ for a Gell-Mann-Zweig quark with charge $Q = 2/3$. The ϕ-angle is the angle between the quark jet and the γ-momentum shown in Fig. 1. Cuts are specified by Eq. (7). Separately shown are the interference term (-•-•-), non-interference term (- - -) as defined by (4b) and their sum (——).

Fig. 3 Same as Fig. 2) for $Q = 1/3$. The result for $Q = -1/3$ is obtained by $\phi \to \pi + \phi$.

Fig. 4 Same as Fig. 2 for $\langle Q\rangle = 2/3$ but $Q^2_{eff} = 1$ (- - -), 1/9(-•-•-) and 4/9(——). The first two examples correspond to charge assignments for colored quarks, where $Q_R = Q_G = Q_B$ is not satisfied.

Fig. 5 Superposition of ϕ-distributions. Cuts are specified by Eq. (7). Separately shown are ϕ-distributions for $|Q| = 2/3$(——) and $|Q| = 1/3$(- - -).

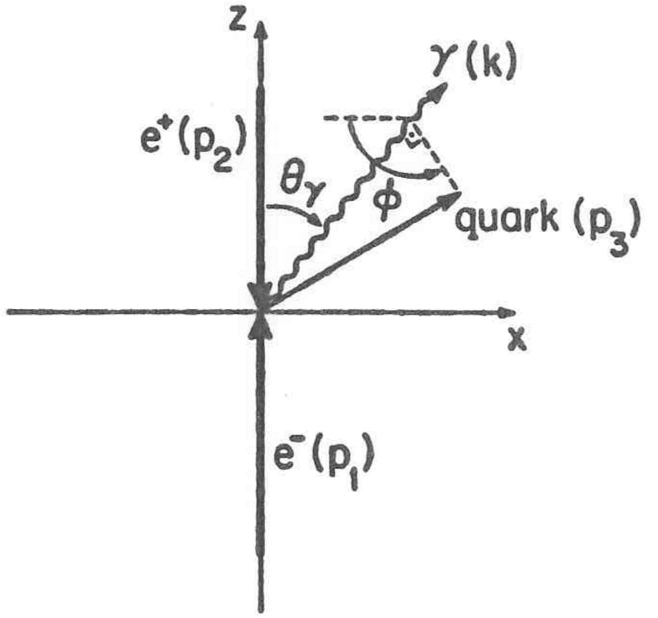

Fig. 1

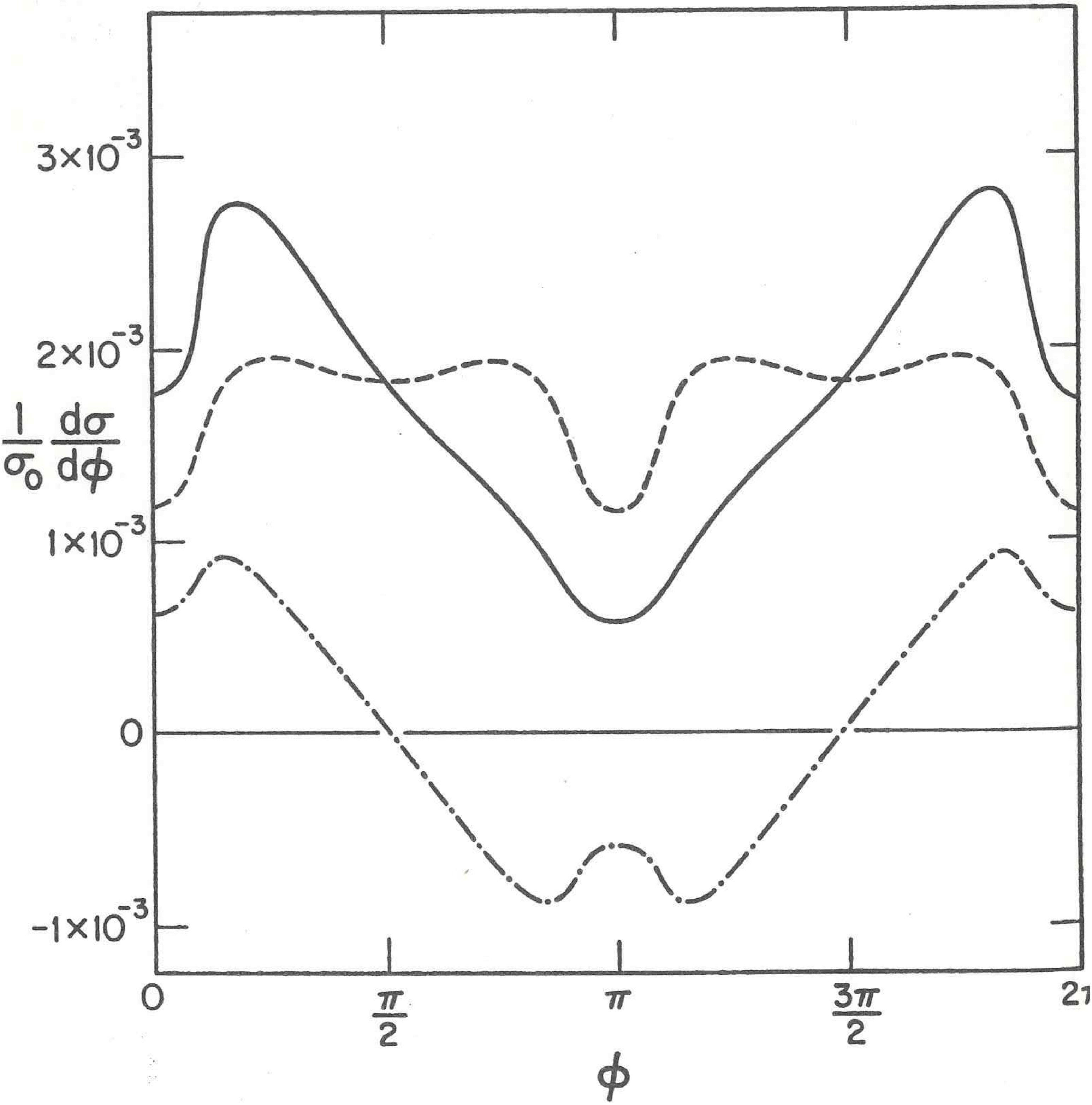

Fig. 2

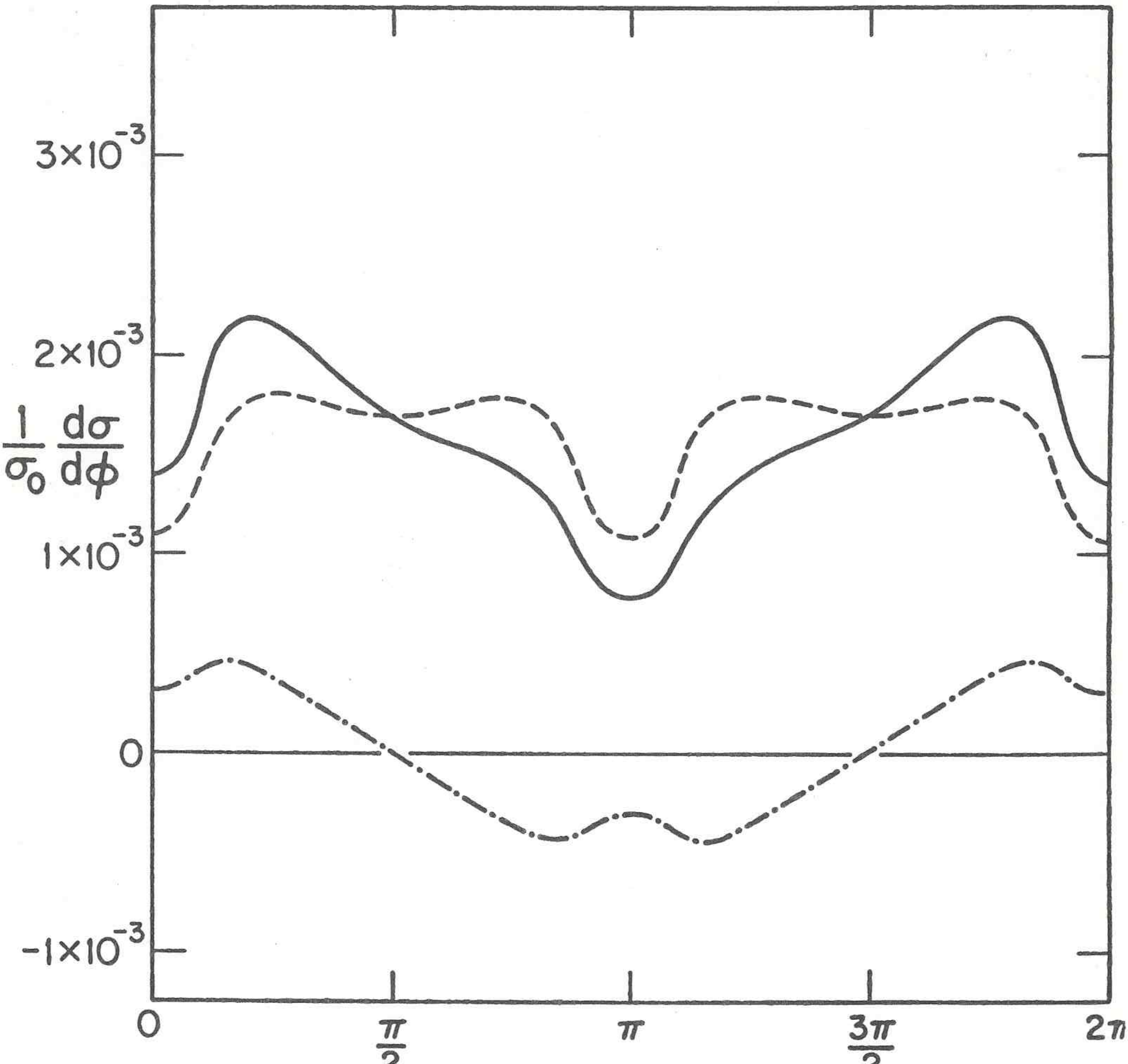

3×10^{-3}
2×10^{-3}
1×10^{-3}
0
-1×10^{-3}
$\frac{1}{\sigma_0}\frac{d\sigma}{d\phi}$
0
$\frac{\pi}{2}$
π
$\frac{3\pi}{2}$
2π
ϕ

Fig. 3

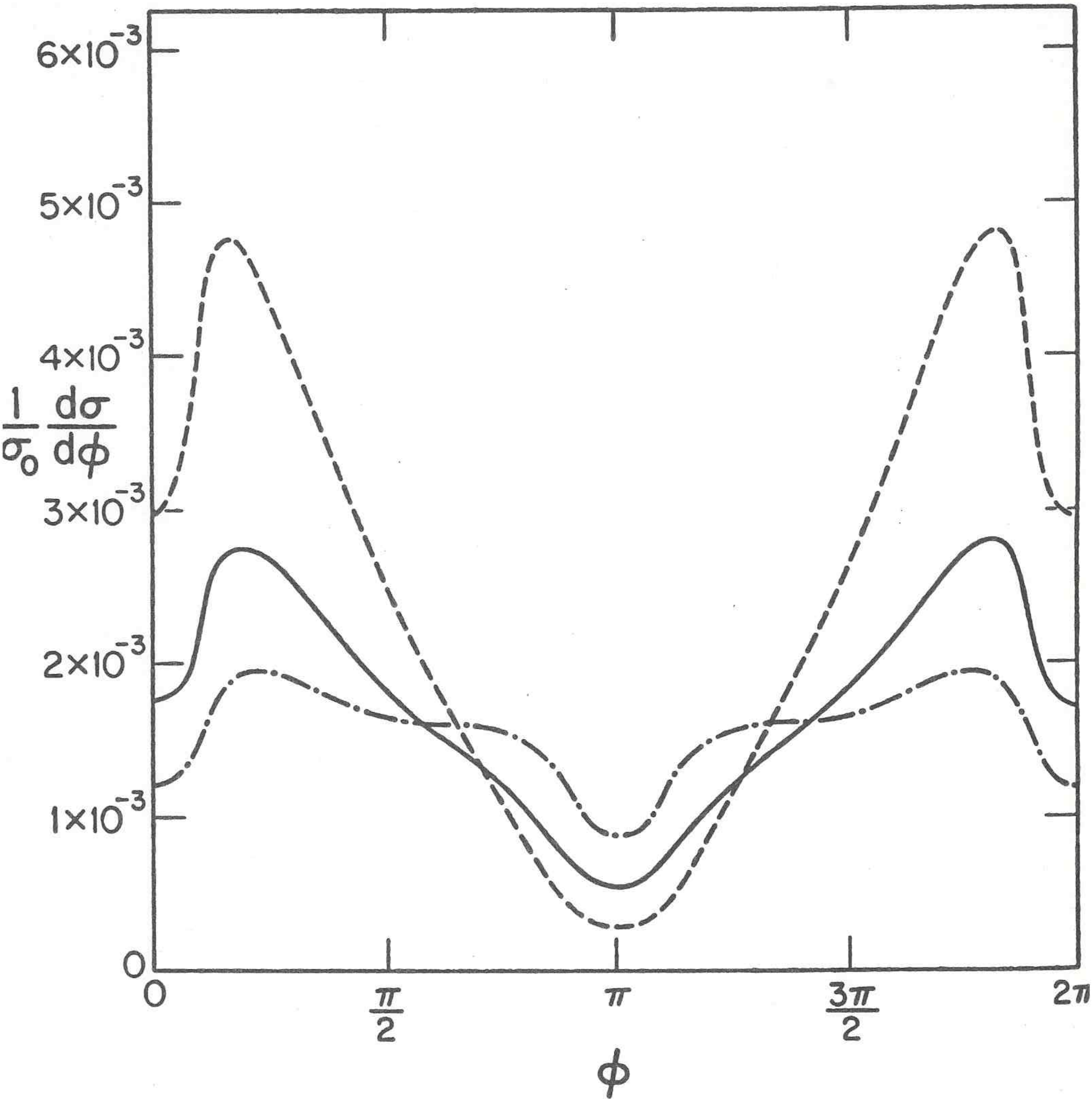

6×10⁻³
5×10⁻³
4×10⁻³
3×10⁻³
2×10⁻³
1×10⁻³
0
$\frac{1}{\sigma_0}\frac{d\sigma}{d\phi}$
0
$\frac{\pi}{2}$
π
$\frac{3\pi}{2}$
2π
ϕ

Fig. 4

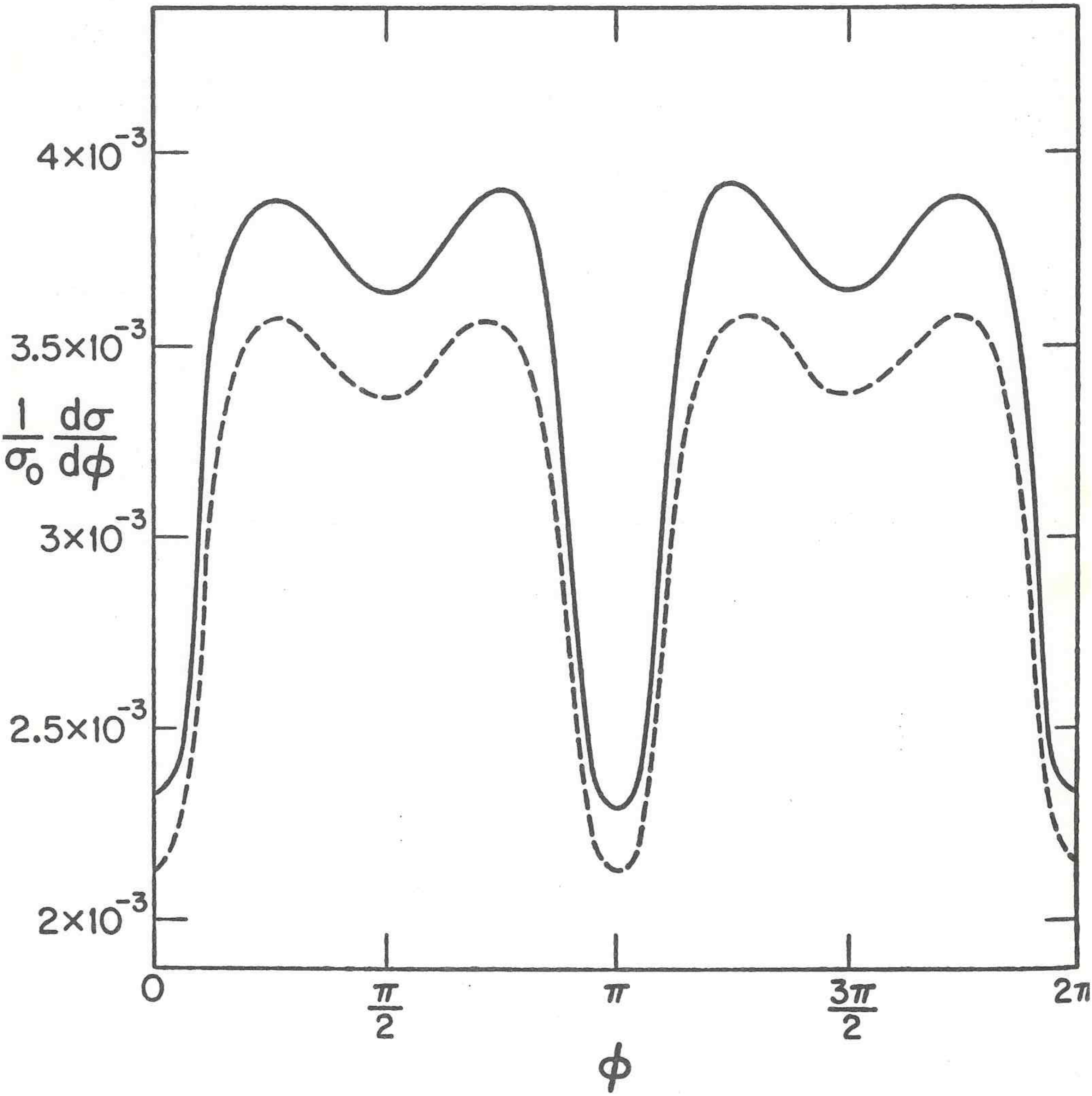
4×10⁻³
3.5×10⁻³
$\frac{1}{\sigma_0}\frac{d\sigma}{d\phi}$
3×10⁻³
2.5×10⁻³
2×10⁻³
0
$\frac{\pi}{2}$
π
$\frac{3\pi}{2}$
2π
ϕ

Fig. 5